ISSN 1505-4675

Technical Sciences

17(2) 2014

Biosystems Engineering
Civil Engineering
Environmental Engineering
Geodesy and Cartography
Information Technology
Mechanical Engineering
Production Engineering

Technical Sciences 17(2), 2014, 105–121

MODELING OF THE STRESS-DEFORMED STATE AND CRACKING INREINFORCED CONCRETE STRUCTURES USING ANSYS MECHANICAL

***Vitaliy Stepanovich Dorofeev*[1], *Vasiliy Mikhaylovich Karpyuk*[2], *Oleksandr Stepanovich Neutov*[1], *Stepan Filipovich Neutov*[2]**

[1] Department of Reinforced Concrete and Masonry Structures
[2] Department of Strength of Materials
Odessa State Academy of Civil Engineering and Architecture, Ukraine

Received 11 June 2013, accepted 5 June 2014, available on line 10 June 2014

K e y w o r d s: concrete beam, stress-strain state, finite-element modeling, ANSYS.

A b s t r a c t

The article presents the results of reinforced concrete beams modeling under short-term loading with the use of the ANSYS Mechanical software. The obtained parameters were compared with the experimental ones. The comparison showed a satisfactory concordance of the parameters. In case of the discrepancies, the authors suggest that they are due to the idealization of material properties and structural model of the finite method. The paper is divided into the following chapters: Introduction, Literature Review, Research Significance, Element Types, Real Constants, Material Properties Modeling, Geometric Modeling, Loads and Boundary Conditions, Cracking and Failure and Conclusions. Each of the five conclusions in the last chapter offers a summary of the presented experimental research.

Introduction

Frequently, providing required load bearing capacity of reinforced concrete beams support areas under complexstress-deformed state is a design driver. Nevertheless, behavior and response of these structure elements in case of high level loads (est. (0.7 – 0.9 V_{ult}) still remain underexplored. That is why, systematic experimental and theoretical research aimed at improvement of the existing and development of modern computational models of support areas in reinforced concrete elements is of essential importance. Various methods have been used to study the response of structural components. Natural experi-

* Correspondence: Stepan Filipovich Neutov, Didrikhsonast., Odessa, 65029, Ukraine, e-mail: neutov.alex@gmail.com, phone +38 0 634 193 089

ments, while producing real time response, are extremely time consuming and quite costly. As for calculation methods, we must mention, that despite all theirefforts (and first of all, price), it is rather unsafe to use them alone for investigation at load levels near 0.9 of ultimate load. Thus, using FEA, such as MacroFe, Ansys, along with natural experiments,is one of the most effective ways to do this task.

In the design of frame concrete structures, it is very important to construct support areas properly. Their combined stress-deformed state makes this task rather difficult. The most common methods used for computational support areas are based on analogies or statistic data and do not describe the real behavior fully.

The aim of this experimental research is to study combinedstress-deformed state of reinforced concrete beams support areas using finite element modeling with ANSYS Mechanical. Authors intended to investigate possibility of modeling the multifactor experiment, and, at the same time, to focus on the behavior of RC beams support areas, shear cracking, stress distribution in shear and longitude reinforcement under short-term loading.

Material and methods

The data presented herein are basis for the five-factor three-level experimental investigation of reinforced concrete beams support areas under steady loading. Full-sized Hartley-5-type experiment plan includes 27 series. Due to

Table 1

Plan of experiment

Series N	Natural values of the factors				
	a/h_0	C, MPa	Shear reinf. at support sect. [%]	Bottom longt. reinf. [%]	Top longt. reinf. [%]
17	3	C20/25	0.0029 (2Ø4 mm)	0.0176 (2Ø14 mm)	0.0090 (2Ø10 mm)
18	1	C20/25	0.0029 (2Ø4 mm)	0.0176 (2Ø14 mm)	0.0090 (2Ø10 mm)
19	2	C30/35	0.0029 (2Ø4 mm)	0.0176 (2Ø14 mm)	0.0090 (2Ø10 mm)
20	2	C12/15	0.0029 (2Ø4 mm)	0.0176 (2Ø14 mm)	0.0090 (2Ø10 mm)
21	2	C20/25	0.0045 (2Ø5 mm)	0.0176 (2Ø14 mm)	0.0090 (2Ø10 mm)
22	2	C20/25	0.0016 (2Ø3 mm)	0.0176 (2Ø14 mm)	0.0090 (2Ø10 mm)
23	2	C20/25	0.0029 (2Ø4 mm)	0.0230 (2Ø16 mm)	0.0090 (2Ø10 mm)
24	2	C20/25	0.0029 (2Ø4 mm)	0.0129 (2Ø12 mm)	0.0090 (2Ø10 mm)
25	2	C20/25	0.0029 (2Ø4 mm)	0.0176 (2Ø14 mm)	0.0129 (2Ø12 mm)
26	2	C20/25	0.0029 (2Ø4 mm)	0.0176 (2Ø14 mm)	0.0058 (2Ø8 mm)
27	2	C20/25	0.0029 (2Ø4 mm)	0.0176 (2Ø14 mm)	0.0090 (2Ø10 mm)

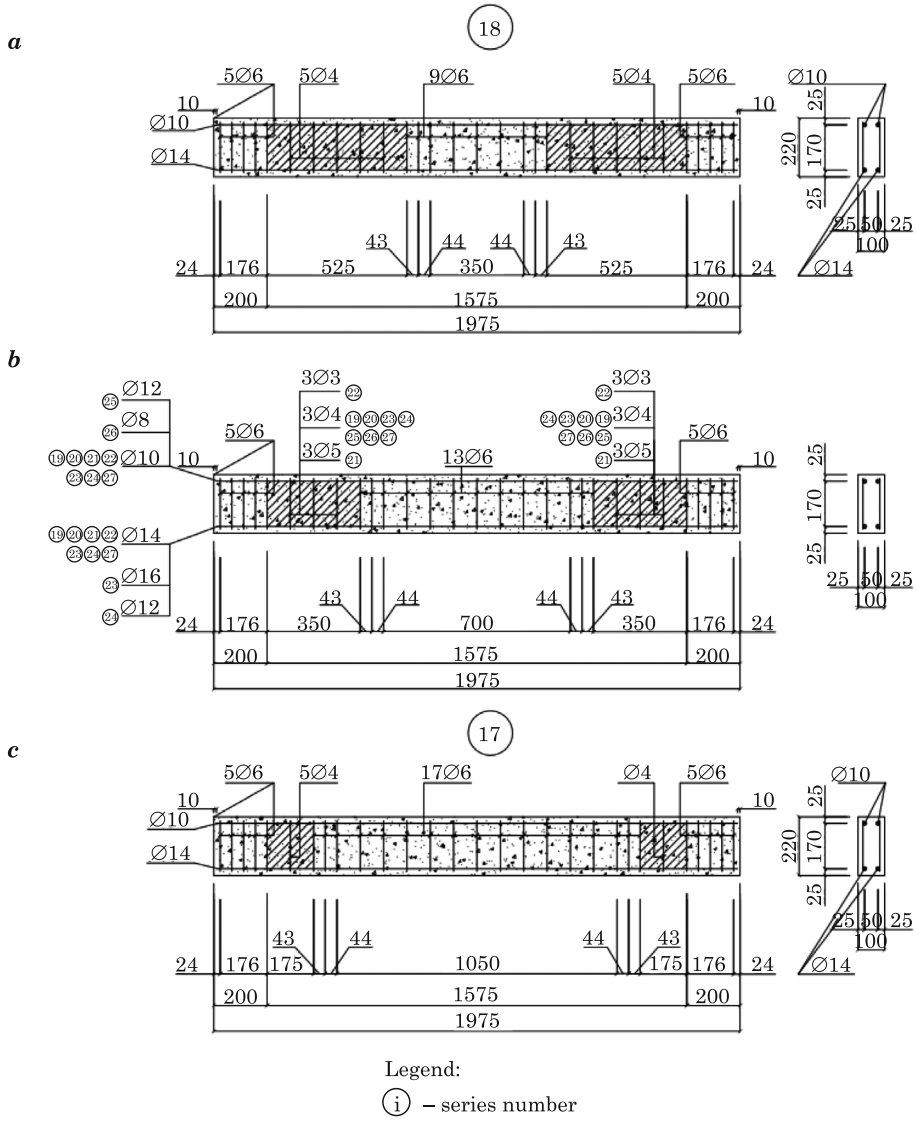

Fig. 1. Beam design: *a* – 18 series, *b* – 19–27 series, *c* – 17 series

considerable complexity of the long-time experiment we decided to use series from 17 to 27 with only one factor variation at one series. Beams of all series are designed to getdestroyedalong support areas. Experimental plan with a description ofexperimental factors and variation levels is shown in Table 1.

Construction scheme of authors' experimental RC beam (DOROFEYEV et al. 2010, 2012) used as calibration model is shown in Figure 1. Simplified scheme that was used to simulate the experimental beam is shown in Figure 2.

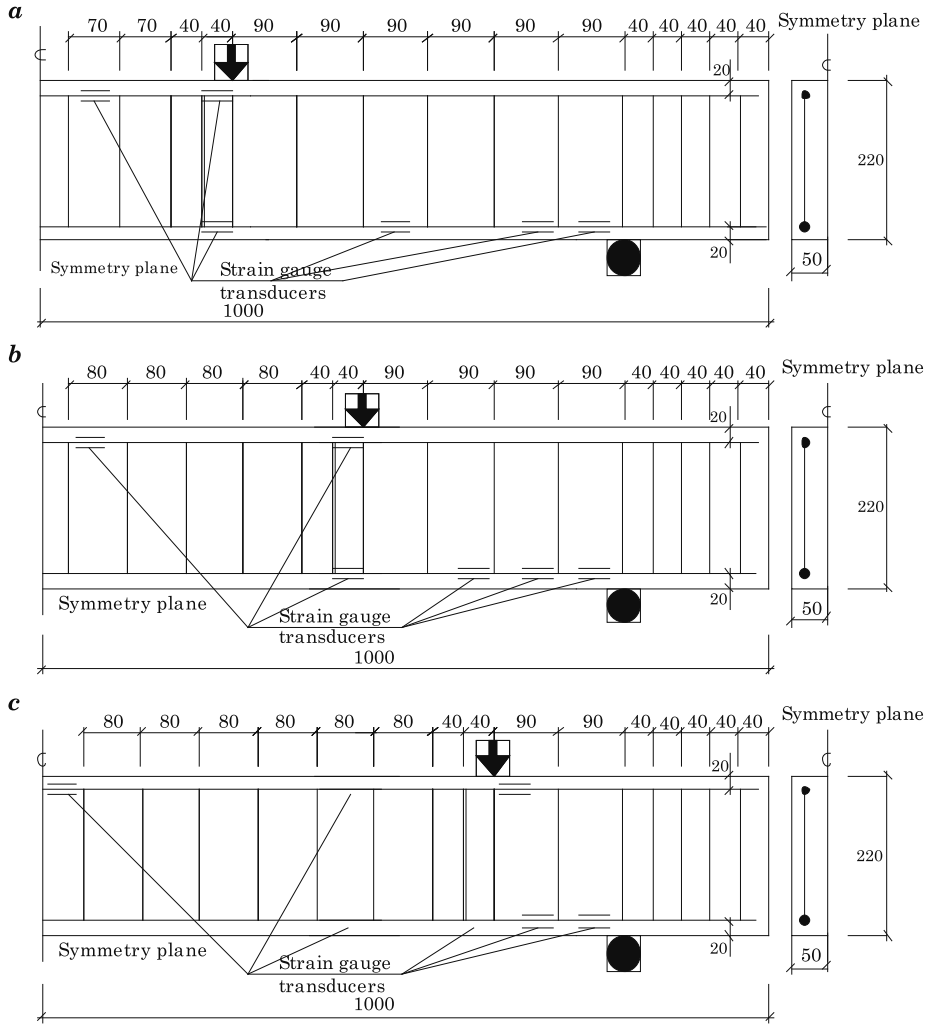

Fig. 2. Model design andstrain gauge transducer scheme: *a* – 18 series, *b* – 19–27 series, *c* – 17 series

The element types for this model are shown in Table 2. The Solid 65 element was used to model the concrete. This element is capable of plastic deformation, cracking in three orthogonal directions, crushing, creep and shrinkage. A Solid 45 element was used for steel load plates and supports of the beam. Both these elements have eight nodes with three degrees of freedom at each node. A Link8 element was used to model steel reinforcement. This is 3D spar element and it has two nodes with three degrees of freedom. Also, it is capable of plastic deformation.

Table 2

Elements and real constants used for model

No	Purpose	Element type	Real constants			
1	concrete	solid 65	rebar direction	*x*	*y*	*z*
			reinf. material	0	0	0
			ρ, %	0	0	0
			orient. angle	0	0	0
			orient. angle	0	0	0
2	bottom longitude reinforcement	link 8	cross-sect. area [m^2]		1.702E-4	
			initial strain		0	
3	top longtitudereinforcement	link 8	cross-sect. area [m^2]		0.785E-4	
			lnitial strain		0	
4	shear reinf. in pure flexure zones	link 8	cross-sect. area [m^2]		0.2827E-4	
			initial strain		0	
5	shear reinf. in support areas	link 8	cross-sect. area [m^2]		0.1257E-4	
			initial strain		0	

Real constants for this model are shown in Table 2. Solid 65 elements requireconstants for rebar assuming a smeared model. In that case, valuesfor Material Number (refers to material model), Volume Ratio and Orientation Angles should be set. Value of zero isentered for all real constants, because discrete reinforcement model is used. For shear, top and bottom reinforcement cross sectional areas and initial strain are defined.

Parameters needed to define material models are shown in Table 3. Complex material model for each element is needed (ANSYS theory reference). The Solid 65 element requires linear isotropic and multilinear isotropic material properties to properly model concrete. The multi-linearisotropic material uses the vonMises failure criterion along with Willam and Warnke model (WILLAM, WARNKE 1974). Modulusof elasticity and Poisson's ratio were assumed according to C20/25 concrete properties. The uniaxial compressive stress-strain relationship for the concrete was obtained using the following equations (DBN – V.2.6-98:2009) with parameters for C20/25 concrete:

$$\sigma_c = f_{(ck)} \sum_{k=1}^{5} a_k \left(\frac{\varepsilon}{\varepsilon_{bR}} \right)^k \tag{1}$$

where

$f_{(ck)}$ – design value of concrete compressive strength;

a_k – the coefficients of the polynomial depending on the parameters, which are used to describe the stress-strain curve;

ε – concrete strain deformation;

ε_{bR} – concrete strain deformation corresponding to the maximum stress value.

Table 3

Material models

Material No	Material	Element type	Material properties		
1	concrete	solid 65	linear isotropic		
			E_x, MPa	3×10^4	
			V_{xy}	0.2	
			multilinear isotropic		
			point num.	ε	σ, MPa
			1	0.000246	7.65
			2	0.000492	15.3
			3	0.00102	19.3
			4	0.00181	25.2
			5	0.00324	13.2
			6	0.00420	5.10
			concrete		
			const1	1	
			const2	0.9	
			const3	0.9	
			const4	51.0	
			const5	-1	
2	support and load plates	solid 45	linear isotropic		
			E_x, MPa	2×10^5	
			υ_{xy}	0.3	
3	longitude reinf.	link 8	linear isotropic		
			E_x, MPa	2×10^5	
			υ_{xy}	0.3	
			multilinear isotropic		
			point num.	ε	σ, MPa
			1	0.00125	250
			2	0.0025	495
			3	0.025	500
4	shear reinf. in pure flexure zones	link 8	linear isotropic		
			E_x, Mpa	2×10^5	
			υ_{xy}	0.3	
			bilinear isotropic		
			yield stress	240	
			tang mod.	145	
5	shear reinf. in support areas	link 8	linear isotropic		
			E_x, MPa	2×10^5	
			υ_{xy}	0.3	
			bilinear isotropic		
			yield stress	410	
			tang mod.	145	

Implementation of Willam and Warnke concrete model requires nine constants to be defined:

1. Shear transfer coefficients for an open crack.
2. Shear transfer coefficients for a closed crack.
3. Uniaxial tensile cracking stress.
4. Uniaxial crushing stress (positive).
5. Biaxial crushing stress (positive).
6. Ambient hydrostatic stress state for use with constants 7 and 8.
7. Biaxial crushing stress (positive) under the ambient hydrostatic stress state.
8. Uniaxial crushing stress (positive) under the ambient hydrostatic stress state.
9. Stiffness multiplier for cracked tensile condition.

Concrete failure surface is described with the following equation

$$\frac{1}{z}\frac{\sigma_a}{f_{cu}} + \frac{1}{r(\Theta)}\frac{\tau_a}{f_{cu}} = 1 \tag{2}$$

where:

f_{cu} – uniaxial compressive strength;
z – apex of the surface;
δ_a, τ_a – average stress components;
Θ – lode angle;
$r(\Theta)$ – quantity, which indicates the locus of the boundary of the stress surface in the deviatoric stress plane.

The reinforcement elements require linear isotropic andmultilinearisotropic material models to be defined. Material of steel load plates and supports of the beam requires only linear isotropic material model.

Concrete, load plates and support element were modeled using volume elements. And the reinforcement was modeled using spar elements. Experimental beam hadtwo symmetry planes and therefore only one quarter of the beam was modeled. Finite element model of concrete and reinforcement with mesh size of 1 cm are shown in Figure 3.

Displacement boundary conditions must be set to constrain the model. To model the symmetry, nodes on the plane must be constrained in the perpendicular direction (UX = 0 and UZ = 0 constraints). The support was modeled in such a way that a roller was created. A constraint in the UY and UZ (applied as constant values of 0) directions was given to the single line of nodes on the plate. The one tenth of the actual force, F, applied across its centerline at the each node. Main calculation parameters are shown in Table 4.

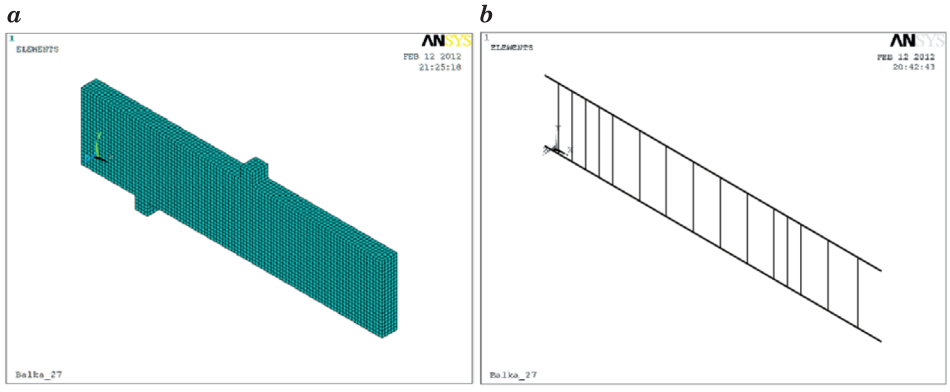

Fig. 3. Mesh of the whole beam (*a*) mesh of the reinforcement (*b*)

Table 4

Calculation options

Main parameters	
Analysis type	Static
Displacement control	big displ.
Prestress effects	off
Time at the end of loadstep	P
Number of substeps	10^6
Automatic time stepping	on
Nonlinear alghoritm and convergence criteria parameters	
Line search	on
Equiv. Plasric strain	1.0
Full Newton-Rapson option with unsym. matrices	on
Maximum number of iterations	10
Element from control	off
Checking elements	No
Convergence criteria	forces
Tolerance	0.5

Results and Discussion

Crack modeling along with cracking of experimental beam for the most characteristic stages of loading is shown in Figure 4. Ultimate, normal and inclined cracking loads for beam series (17-27) obtained both from natural experiment and modeling using ANSYS are shown in Table 5. We must state, firstly, that cracking load for the model is smaller than for experimental beam;

secondly, that cracks in the model develop more intensively, due to cracking criteria used in Willam-Warnke model. Experiment results indicate that cracking process, both in a simulated beam and corresponding experimental one, begins from the pure flexure zone at the load level close to 0.3 V_{ult}. Inclined cracks appear in the support areas later, at the loads about. This process is significantly affected by concrete class, percentage of transversal and longitude reinforcement.

Comparing whole cracking pattern in model and experimental beam at the load about 0.8 V_{ult} we must state their similarity, as well as equal crack heights. Figures 5 and 6 show the experimental values of midspan deflections and longitude reinforcement deformations of the series 22 and the results of their simulations, where 22–1(1) means "22 series, 1st beam, left side of experimen-

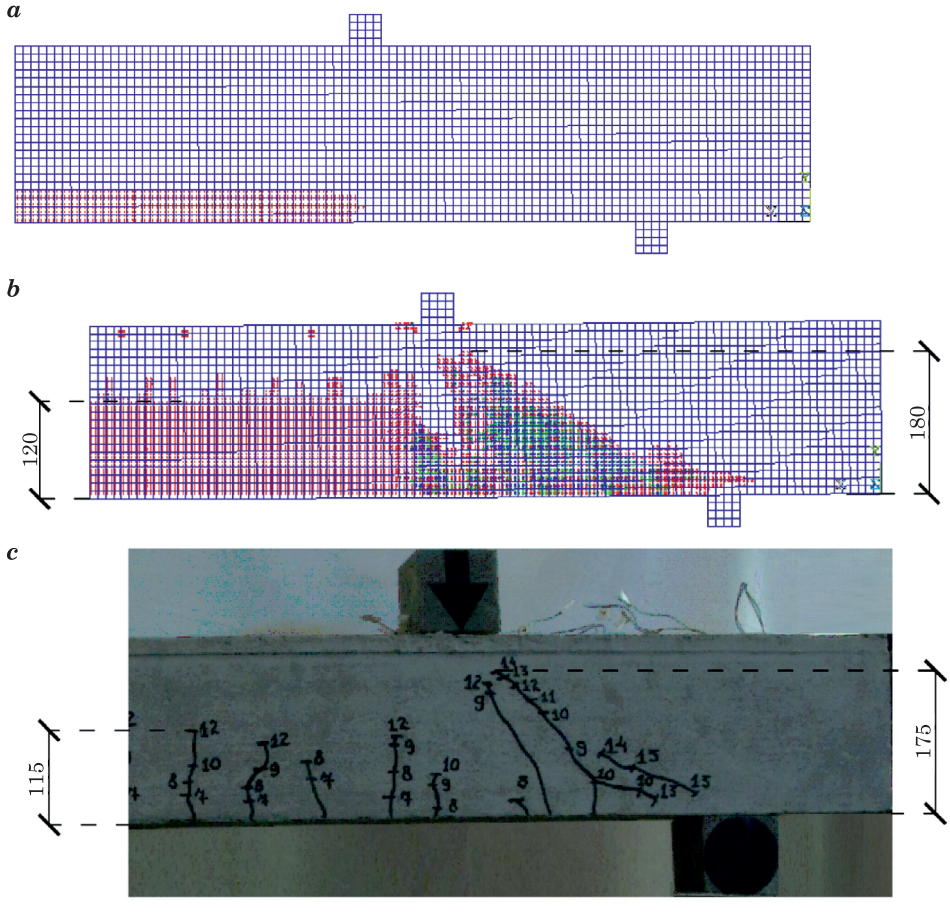

Fig. 4. Modeling of crack at load levels: 0.3 V_{ult} (*a*), 0.8 V_{ult} (*b*); appearance and crack opening in the experimental sample (*c*)

tal beam" and 22–1(2) means "22 series, 1st beam, right side of experimental beam" respectively. It is obvious, that up to, congruence is more than satisfactory. Further increasing discrepancy is due to method limitations.

Table 5

Failure and cracking loads

Series	Model			Experiment		
	V_{ult} [kN]	$M_{(cr)}$ (normal cracks at pureflexure zone) [kNm]	$F_{(cr)}$ (inclined cracks at the support area) [kN]	V_{ult} [kN]	$M_{(cr)}$ (normal cracks at pureflexure zone) [kNm]	$F_{(cr)}$ (inclined cracks at the support area) [kN]
0–17	147	18	20	140	20	30
0–18	60	46	50	64	50	70
0–19	120	26	27	116	27	65
0–20	75	15	28	72	28	45
0–21	86	25	33	96	33	48
0–22	81	22	32	82	32	40
0–23	96	25	33	100	33	48
0–24	65	21	26	72	26	48
0–25	86	25	30	89	30	48
0–26	86	23	30	84	30	40
0–27	86	23	30	86	30	48

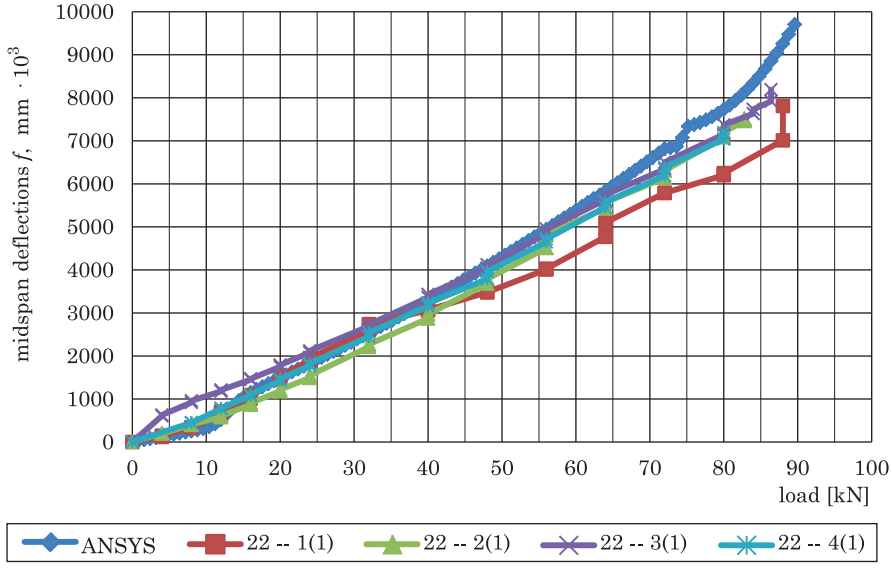

Fig. 5. Calculated and experimental values of beam midspan deflections

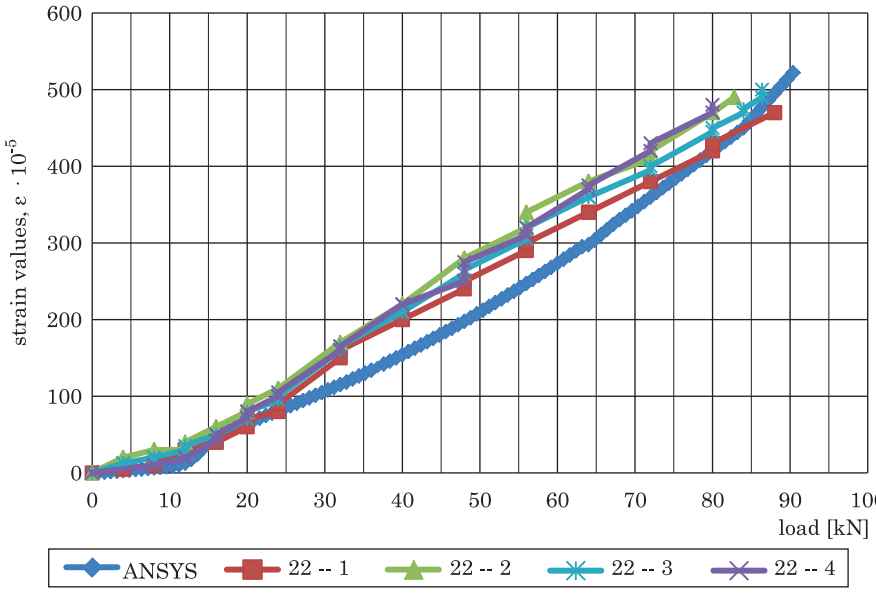

Fig. 6. Calculated and experimental strain values in bottom rebar sat mid span

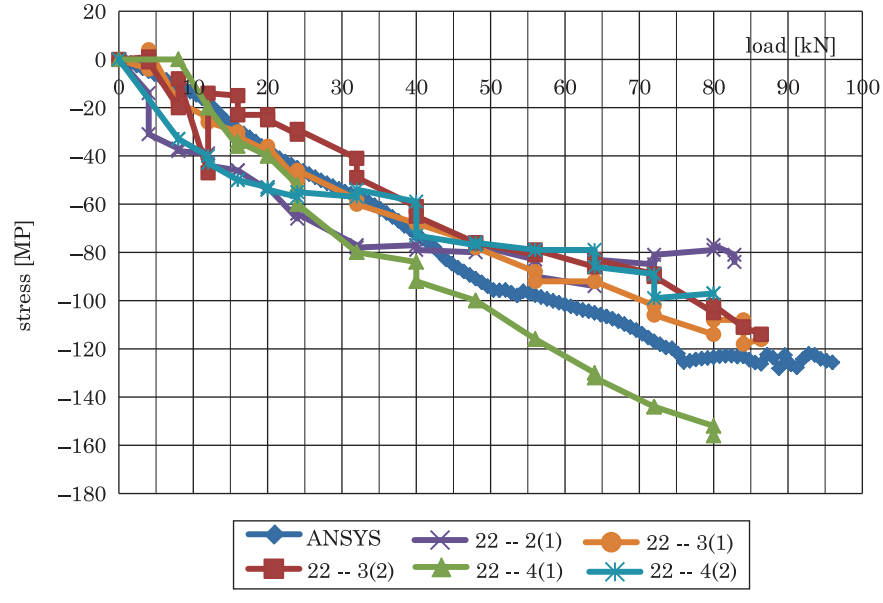

Fig. 7. Calculated and experimental stress values in top reinforcement near the load plate (at the end of support area)

Calculated values of longitude reinforcement stresses along with modeled values are shown in Figures 7–10. Experimental values have been obtained byprocessing the strain gauge transducer chain data, located on bottom and top longitude reinforcement both in pure flexure zone and support areas. It is fair to say that, in total, congruence of experimental and modeled stress-deformed state of top reinforcement is stable (Fig. 6 and 7).

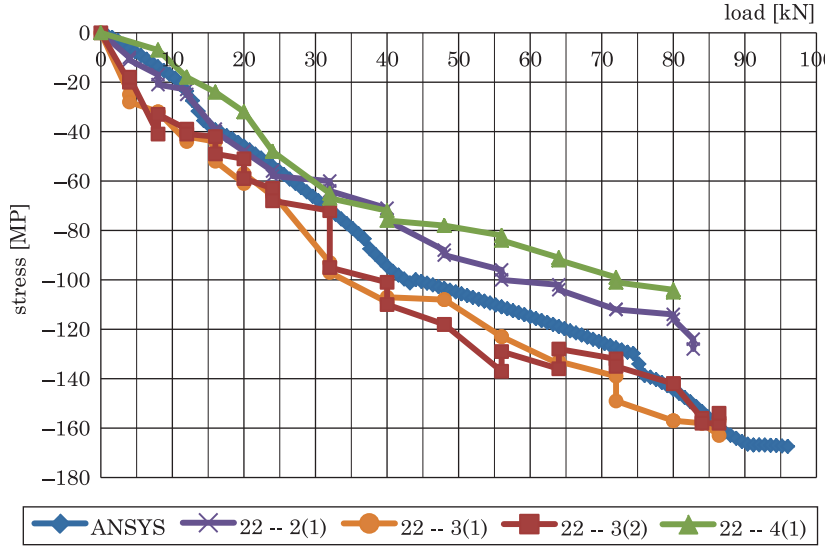

Fig. 8. Calculated and experimental stress values in top reinforcement in pure flexure zone

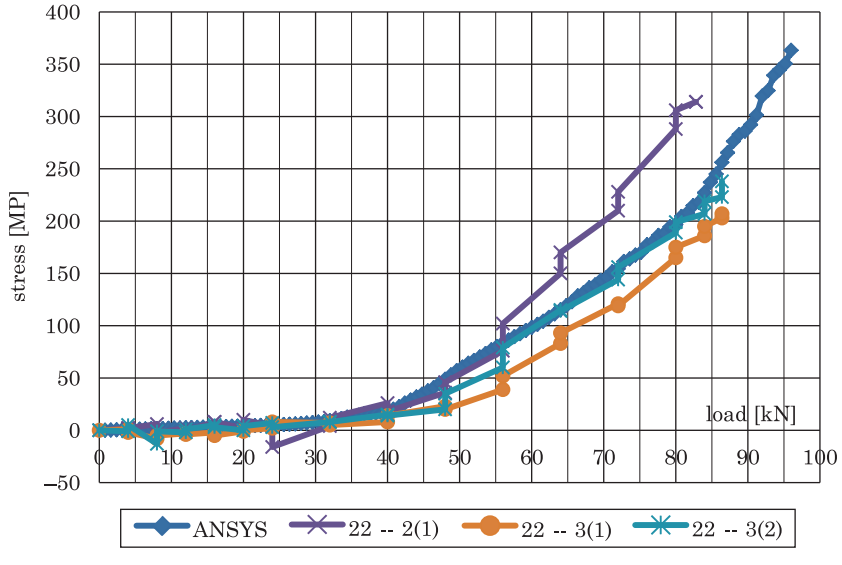

Fig. 9. Calculated and experimental stress values in bottom reinforcement near the support hinge

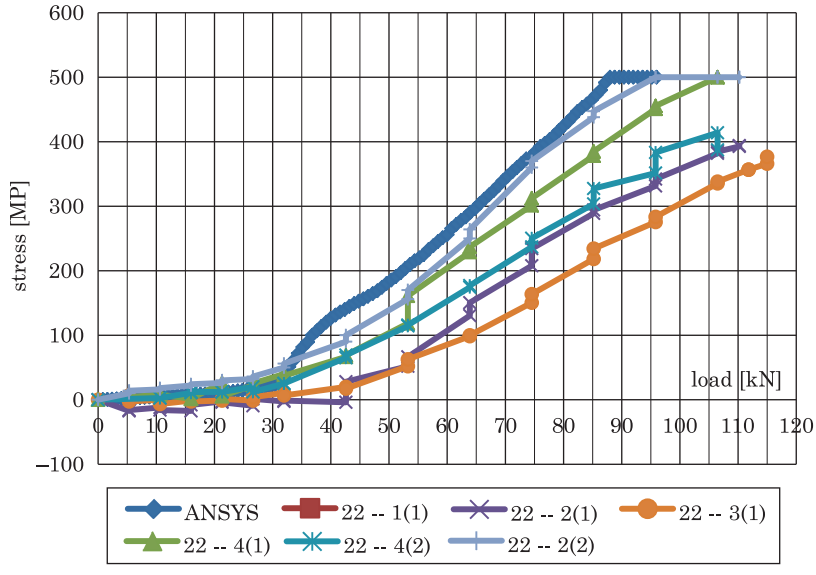

Fig. 10. Calculated and experimental stress values in bottom reinforcement at apoint located at a distance of 9 cm from the support (at the mouth of the critical inclined crack)

As for bottom reinforcement, they differ more significantly. In a greater degree this concerns pure flexure zone on loading, which is close to failure. Under these load levels cracking process in model is like an avalanche, leading to substantial strain growth. To a smaller extent it concerns bottom reinforcement in support areas, although model strain rate is biggerthan in natural beams. And, vice versa, modeled top reinforcement strain is less than experimental ones.

Stressed state of shear reinforcement was studied according to scheme, shown in Figure 11. Relations between load and modelled stresses in shear reinforcement bars in the support areas are shown in Figures 12, 13, 14.

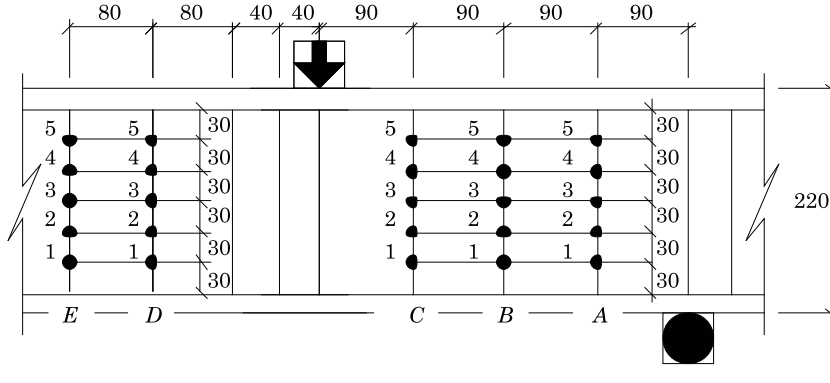

Fig. 11. Characteristic points of the shear reinforcement in the bars *A, B, C* in the support areas, *D, E* – in pure flexure zone

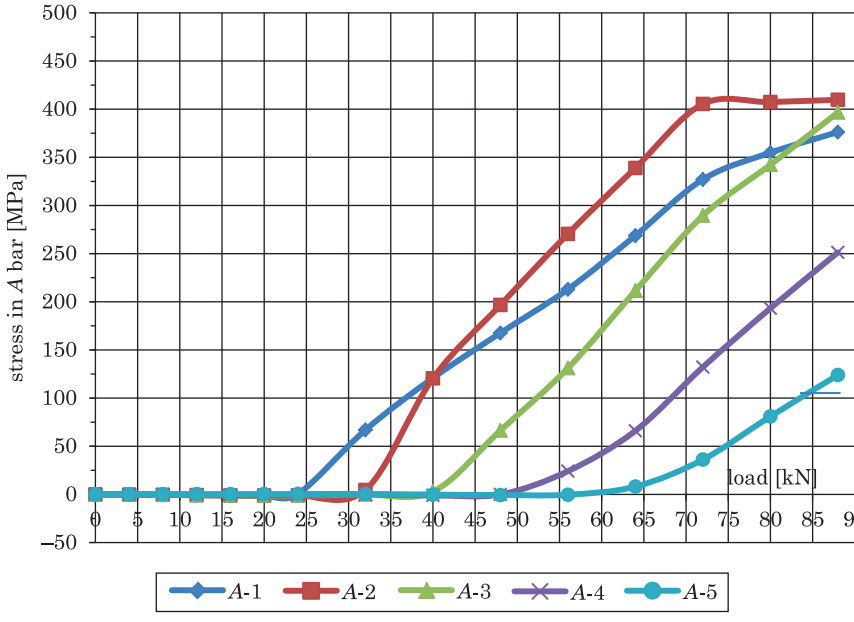

Fig. 12. Force-stress graph for the charecteristic points of the rebar *A*

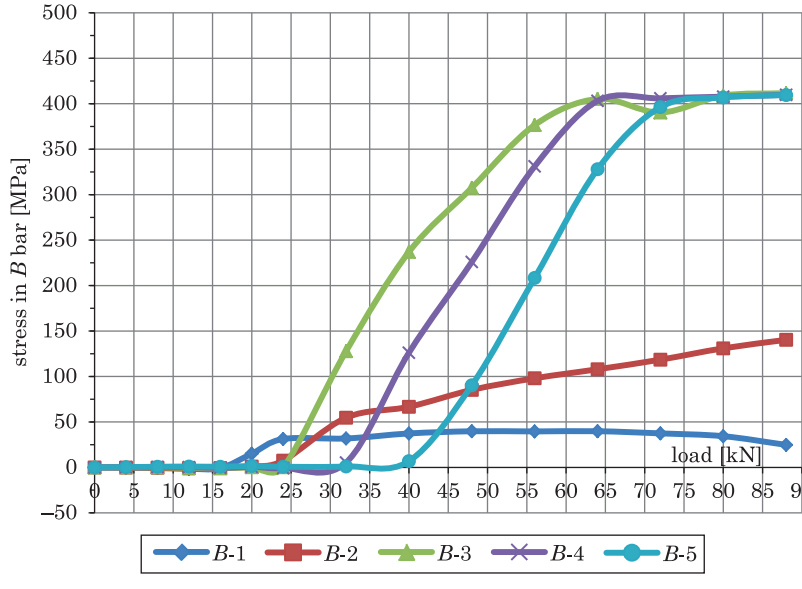

Fig. 13. Force-stress graph for the charecteristic points of the rebar *B*

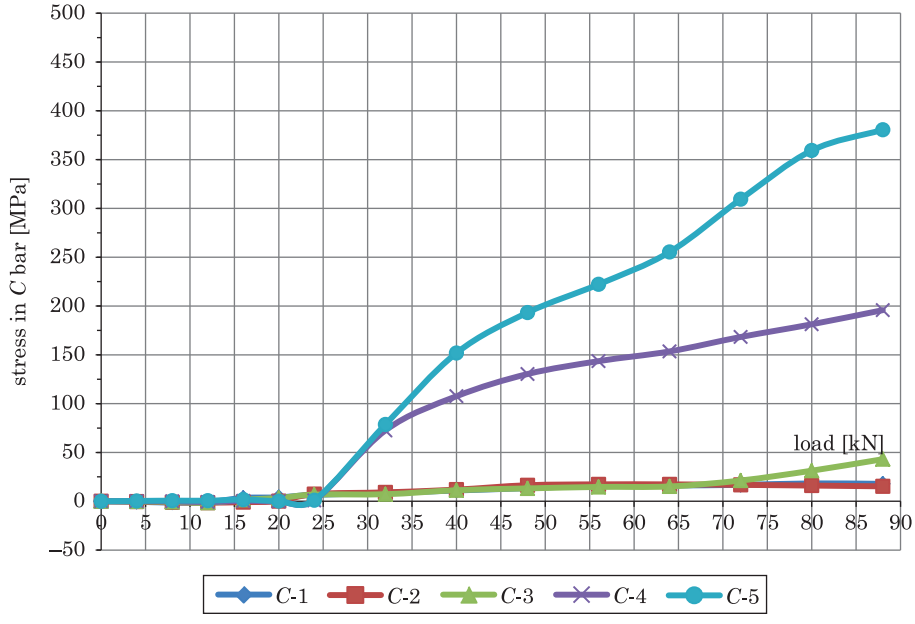

Fig. 14. Force-stress graph for the charecteristic points of the rebar *C*

As we can see, results shown in Figure 12, indicate that stresses in shear rebar *A* are unevenly distributed.Initially, the lowest point 1 is "turned on", then point 2, etc. Stresses in 5th point begin to grow sugnificantly only with load level about 0.75 V_{ult}. The most stressed point in *A* shear rebar is point 2. At load level about 0.80 V_{ult}, stresses in that point reach the yield strength. Point 1 is the second most stressed point, point 3 – the third one – its stresses reach yield strength at the time of failure.

Shear rebar *B*, which is located near midspan (Figure 13), is the most heavily loaded, as stresses reach yield strength in 3 of 5 of his characteristic points. It should be noted, that in these points stresses reach yield strength at load level about. Ultimate stresses in points 1, 2 reaches only 30 and 140 MPa respectively.

Shear reinforcement bar *C*, adjacent to the pure flexure zone, is the least loaded. Almost the entire height (points 1, 2, 3) stresses in their points are less than 50 MPa. Point 4 stress reaches 200 MPa. The most heavily loaded point in this rebar is point 5 (380 MPa), which is very close to the yield point. Modeling results which are shown in Figures 12–14, allow to indicate the direction and area of probable cracks occurrence (Figure 15). In order to do that we can draw a line across points in shear bars where stresses reach ultimate values. Cracking in the support area of experimental beam along with the first principal strain color map is shown in Figure 16. The results presented here indicate that modeled crack patterns practically coincide with the experimental ones.

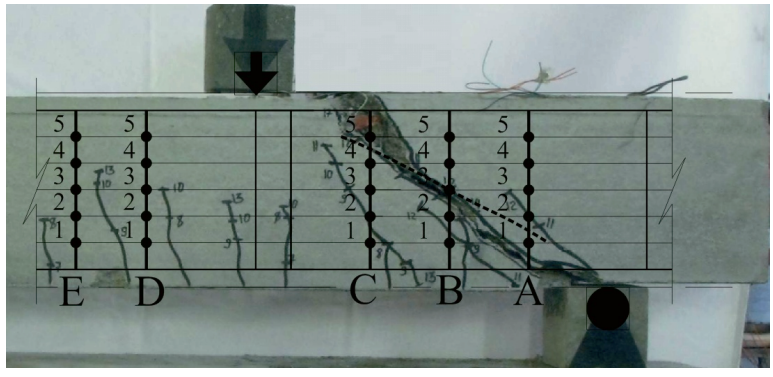

Fig. 15. Cracking and failure of experimental beam support area

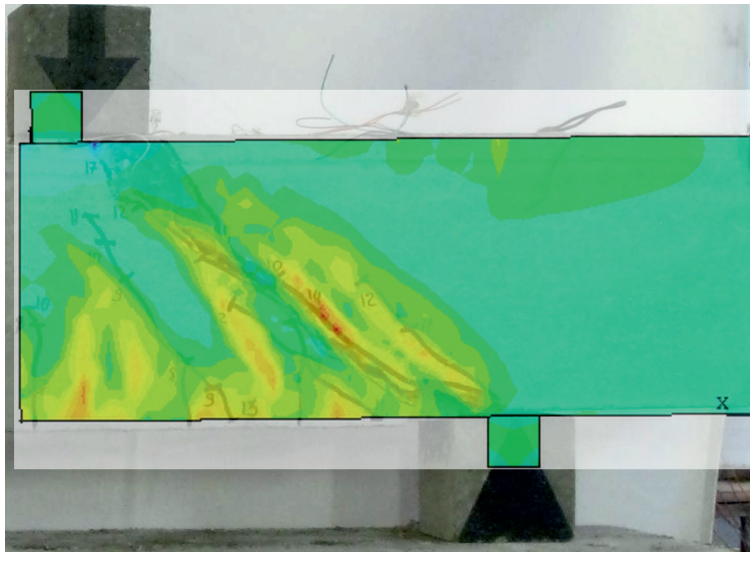

Fig. 16. Cracking in the support area along with the first principal strain color map

Conclusions

1. Failure mechanism modeling using FEA Ansys shows reliable results while received failure load is very close to experimental.

2. Modeled cracking load is also close to experimental. At the same time, it should be noted that cracking pattern in model is rather simplified compared to natural beams and crack growth rate in model is greater than in experimental beam due to restrictions of Willam-Warnke concrete model used in Ansys.

3. Modeled deflections and strains are almost the same as the experimental ones up to.

4. The stresses in top and bottom reinforcement bars received through modeling showed very good agreement and confirmed by direct measurements, actual cracking process in the test beams, as well as other experimental parameters. Discrepancies are due to the idealization of material properties and structural model of the finite element method.

5. Modeling of shear reinforcement provided that good agreementaccording to other parameters of stress-deformedstate can provide valuable data on the growth and change in the pattern of stresses in the shear reinforcement bars, which are difficult to get with a direct experiment. These data are indirectly confirmed as the development of the main crack in the experimental beam.

6. Modeling of the stress-deformed state of researched elements using FEA ANSYS unlike other approved local software systems (in particular, "Lyra", "SCAD", "Monomakh") gives an opportunity to predict the formation and development of both normal and inclined cracks on support areas of bending elements, and the possible mechanism of their failure.

References

ANSYS theory refence. 12th ed, SAS IP, Inc.

DBN – V.2.6-98:2009. Concrete and reinforced concrete structures. Fundamentals. 2011. Ukranian State Bulding Code. Kyiv, The Ministry of Regional Development and Construction.

DOROFEYEV V.S., KARPIUK V.M., NEUTOV A.S. 2010. *Experimental study of reinforced concrete beams support sections under steadyloading*. Journal of Odessa State Academy of Building and Architecture, 38, 255–262.

DOROFEYEV V.S., KARPIUK V.M., NEUTOV A.S.2010. *On the influence of structural factorson the carrying capacity of bendable concrete elements*. Journal of Odessa State Academy of Building and Architecture, 39(1): 186–199.

DOROFEYEV V.S., KARPIUK V.M., NEUTOV A.S. 2012. *On the simulation of the stress-deformed state of reinforced concrete beams in the FEA Ansys Mechanical*. Journal of Odessa State Academy of Building and Architecture, 46: 75–86.

KACHLAKEV D.I., MILLER T. H., YIM S., CHANSAWAT K., POTISUK T. 2001. *Finite Element Modeling of Reinforced Concrete Structures Strengthened With FRP Laminates*. Final Report FHWA-OR-RD-01-17, SPR 316, 111 pages plus appendices, United States Department of Transportation, Federal Highway Administration and Oregon DOT, Salem, Oregon.

SAIFULLAH I., NAZIR-UZ-ZAMAN M., UDDIN S.M. *Experimental and Analytical Investigation of Flexural Behavior of Reinforced Concrete Beam*. IJET, 11(02): 188–196.

VASUDEVAN G., KOTHANDARAMAN S. 2011. *Parametric study on Nonlinear Finite Element Analysis on flexural behaviour of RC beams using ANSYS*. International Journal of Civil and Structural Engineering, 2(1): 98–11.

WILLAM K.J., WARNKE E.P. 1974. *Constitutive model for triaxialbevior of concrete*. Proceedings of international associations of bridge and structural engeneering conference, Vol. 19, ISMES, Bergamo, Italy, pp. 174–191.

WOLANSKI A. J., B.S. 2004. *Flexural behaviour of reinforced and prestressed concrete beams using finite element analysis*. Master's Thesis, Marqutte University, Milwaukee, Wisconsin, p. 87.